Correlation of Particulate Dispersion Stability with the Strength of Self-Assembled Surfactant Films

Joshua J. Adler,[†] Pankaj K. Singh,[†] Alex Patist,[‡] Yakov I. Rabinovich, Dinesh O. Shah,[‡,||] and Brij M. Moudgil*,[†]

Engineering Research Center for Particle Science & Technology and Center for Surface Science & Engineering, Department of Materials Science and Engineering, Department of Chemical Engineering, and Department of Anesthesiology, University of Florida, Gainesville, Florida 32611

Received March 11, 2000. In Final Form: June 22, 2000

Self-assembled surfactant films at the solid/liquid interface are investigated as a means to impart stability to nanoparticulate suspensions in extreme environments. Resistance to elastic deformation of the surface surfactant structures is proposed as the primary stabilization mechanism. There exists a critical concentration of surfactant, above which, repulsive forces between coated surfaces are measured and particle stability occurs. This concentration does not correspond to the critical hemimicelle concentration or the bulk critical micelle concentration. Instead, it appears during bilayer formation indicating a possible transition of structure. The effect of alkyl chain length, electrolyte concentration, cosurfactant addition, and substrate on this concentration and the magnitude of the repulsive force demonstrates the similarities between the formation of these self-assembled surfactant surface structures and the formation and stability of bulk micelles.

Introduction

Traditional and emerging technologies such as advanced structural ceramics, controlled drug delivery systems, abrasives for precision polishing, coatings, inks, and nanocomposite materials are increasingly relying on nanoparticulate precursor materials to achieve optimum performance. Concurrently, environmental and safety issues have driven industrial processes toward synthesis and processing in aqueous media. The result has been increased attention to the role of particle size in the dispersion of concentrated (>50 vol %) aqueous particulate suspensions.[1−5]

Electrostatic repulsion is often applied to stabilize homogeneous, low ionic strength suspensions where pH can be controlled in order to provide sufficient surface charge. Considering that the energy imparted to particles during processing or Brownian motion is relatively constant as a function of particle size, but the repulsive energy between particles due to electrostatics decreases proportionally with size, a greater surface potential is needed to disperse nanoparticulates than larger particles. This effect may be great enough that pH adjustment or addition of inorganic dispersant, such as sodium silicate, may not always lead to suspension stability. Furthermore, many processes such as chemical mechanical polishing and crystallization, must operate in extremes of ionic strength, temperature, pH, mechanical force, or high shear rate where electrostatic stabilization alone may not be adequate to prevent agglomeration. Hence, polymeric reagents are more commonly utilized.[6−9]

In concentrated suspensions, relatively large polymeric dispersant molecules may significantly increase the effective volume fraction of the suspension, and hence viscosity, due to the quantity of immobilized liquid in the dispersant coating and the relative high surface area of nanoparticles. To minimize this effect, dispersant molecules should be small and bind as little water as possible while still providing an adequate barrier to agglomeration. Since most polymeric dispersants do not form compact layers at the interface, a relatively large molecule is often used (>10 000 MW) and the increase in effective volume fraction is likely to result in higher viscosity.[9] Additionally, many polymeric dispersants are polyacrylate based and may perform poorly under extremes of pH and ionic strength. These limitations have motivated the search for alternative dispersants to stabilize suspensions in extreme environments and maintain fluidity in concentrated suspensions.

There are a number of necessary criteria that must be met for a molecule to act as a dispersant. The reagent must (i) adsorb to the surface under the given process conditions, (ii) not phase separate or otherwise adhere to the dispersant layer of an approaching particle, and (iii) provide adequate repulsion between particles to prevent agglomeration. Surfactant molecules adsorb at the solid/liquid interface through mechanisms such as electrostatic, hydrogen, hydrophobic, and specific bonding. Criterion (ii) is fulfilled if the hydrophilic moieties of the surfactant

* To whom correspondence should be addressed: Brij M. Moudgil, 205 Particle Science and Technology Bldg., PO Box 116135, Gainesville, FL 32611-6135. Phone: (352) 846-1194. Fax: (352) 846-1196. E-mail: bmoudgil@erc.ufl.edu.

Engineering Research Center for Particle Science & Technology and Center for Surface Science & Engineering.

[†] Department of Materials Science and Engineering.

[‡] Department of Chemical Engineering.

[||] Department of Anesthesiology.

(1) Higashitani, K.; Kondo, M.; Hatade, S. *J. Colloid Interface Sci.* **1990**, *142*, 204.

(2) Hackley, V. A.; Paik, U.; Kim, B.-H.; Malghan, S. G. *J. Am. Ceram. Soc.* **1997**, *80*, 1781.

(3) Hirata, Y. *Ceram. Int.* **1997**, *23*, 93.

(4) Himics, R.; Pineiro, R. *Process Finishing* **1998**, *63*, 8.

(5) Wu, G.; Matijevic, E. *J. Dispersion Sci. Technol.* **1998**, *19*, 903.

(6) Tadros, Th. F. In *The Effect of Polymers on Dispersion Properties*; Tadros, Th. F., Ed.; Academic Press: London, 1982; p 1.

(7) Russel, W. B.; Saville, D. A.; Schowalter, W. R. *Colloidal Dispersions*; Cambridge University Press: Cambridge, 1989.

(8) Reed, J. S. *Principles of Ceramic Processing*, 2nd ed.; John Wiley & Sons: New York, 1995.

(9) Cesarano, J., III; Aksay, I. A. *J. Am. Ceram. Soc.* **1988**, *71*, 1062.

10.1021/la000363c CCC: $19.00
Published on Web 08/12/2000

molecules adsorbed on separate particles interact with each other as demonstrated by the ability of surfactants to stabilize oil-in-water emulsions. It remains, however, to be shown that surfactant layers can produce a barrier to agglomeration that is large enough to disperse inorganic particles in aqueous media. In the remainder of this discussion, the utility of self-assembled surfactant films in the dispersion process will be investigated with specific emphasis placed on their effectiveness in extreme environments, such as high ionic strength.

Surfactant adsorption to surfaces is a phenomenon of critical importance to various industrial processes ranging from ore flotation, lubrication, and paint technology to enhanced oil recovery.[10] The process of and factors affecting surfactant micellization in bulk solutions leading to spherical or cylindrical micelles, bilayers, or bicontinuous phases are relatively well understood.[10] At interfaces, however, the self-assembly process is influenced by additional surfactant−surfactant, surfactant−surface, surfactant−solvent, and solvent−surface interactions, including the free energy of adsorption, roughness, surface heterogeneity, charge, and crystallinity.

Traditionally, adsorption isotherms combined with techniques such as contact angle and zeta potential have been used to delineate the self-assembly behavior of surfactants at the solid/liquid interface.[11−17] More recently, these techniques have been augmented by methods such as fluorescence decay,[18−19] electron spin resonance (ESR),[20−21] Raman spectroscopy,[22] nuclear magnetic resonance (NMR),[23] neutron reflectometry,[24] calorimetry,[25] infrared absorption (FT-IR),[26−27] small angle neutron scattering (SANS),[28] ellipsometry,[29−30] and surface force measurement.[31−34] On the basis of observations made via the above techniques, many important insights into the self-assembly process at surfaces have been made, including a description of hemimicellization processes, critical aggregation numbers, and adsorption kinetics. However, the morphology of self-assembled surfactant structures at the solid/liquid interface remained controversial due to limited direct experimental techniques.

In the past few years, the atomic force microscope (AFM) has been used to directly image surfactant adsorbed at the solid/liquid interface.[35,36] It has been found that there is a strong influence of the surface in controlling the aggregate structure. For example in quaternary ammonium surfactant systems, mica tends to form full cylindrical micelles that meander across the surface with changes in direction corresponding to the mica lattice structure. Amorphous silica, on the other hand, lacks these atomic rows, and as such, full spheres are observed. These structures and their dependence on solution conditions, surfactant type, and time have been investigated by a number of authors.[35−46]

Although past investigations have revealed much about the structure of surfactant films adsorbed on surfaces, very little has been reported on the stability or technological implications of these self-assembled surfactant surface structures. The goal of the present study is to investigate the similarities between the formation and stability of bulk micelles and self-assembled surfactant surface structures and to demonstrate the effectiveness of an adsorbed micelle layer in the stabilization of a suspension.

Experimental Section

Materials. Interparticle forces were measured between a silicon wafer with a 2 μm thick coating of CVD silica (Motorola) or a freshly cleaved mica substrate (S &J Trading Inc.) and the silicon nitride tip of an atomic force microscope cantilever. The roughness of the silica surfaces as measured by atomic force microscopy is less than 0.5 nm root mean square. Triangular oxide sharpened contact mode cantilevers of 0.12 N/m spring constant (200 nm long, thick legged) were obtained from Digital Instruments. Water was produced by a Millipore filtration system and had an internal specific resistance of 18.2 MΩ and less than 7 ppb carbon. Surfactants were obtained from Aldrich Chemical Co. and were at least 99% pure, with the exception of octyltrimethylammonium bromide, acquired from Lancaster Synthesis at 97% purity. All other reagents were provided by Fisher Scientific Inc. and were at least ACS reagent grade. Surfaces (except mica) were cleaned by copious rinsing with acetone, water, NoChromix (concentrated sulfuric acid and oxidizer), and additional water in sequence. Surfaces were cleaned immediately prior to experimentation.

Methods. (a) Surface Force Measurement. Surface force was measured on a Digital Instruments Nanoscope III in a fused

(10) Rosen, M. J. *Surfactants and Interfacial Phenomena*, 2nd ed.; John Wiley & Sons: New York, 1989.
(11) Fuerstenau, D. W.; Healy, T. W.; Somasundaran, P. *Trans. AIME* **1964**, *229*, 321.
(12) Fuerstenau, D. W.; Wakamatsu, T. *Faraday Discuss. Chem. Soc.* **1975**, *59*, 157.
(13) Scamehorn, J. F.; Schechter, R. S.; Wade, W. H. *J. Colloid Interface Sci.* **1981**, *85*, 463.
(14) Scamehorn, J. F.; Schechter, R. S.; Wade, W. H. *J. Colloid Interface Sci.* **1981**, *85*, 479.
(15) Scamehorn, J. F.; Schechter, R. S.; Wade, W. H. *J. Colloid Interface Sci.* **1981**, *85*, 494.
(16) Moudgil, B. M.; Soto, H.; Somasundaran, P. In *Reagents in Mineral Technology*; Somasundaran, P., Moudgil, B. M., Eds.; Marcel Dekker: New York, 1988; Surfactants Science Series Vol. 27; p 79.
(17) Hough, D. B.; Rendall, H. M. In *Adsorption from Solution at the Solid / Liquid Interface*; Parfitt, G. D., Rochester, C. H., Eds.; Academic Press: London, 1983; p 247.
(18) Chandar, P.; Somasundaran, P.; Turro, N. J. *J. Colloid Interface Sci.* **1987**, *117*, 31.
(19) Ström, C.; Hansson, P.; Jönsson, B.; Söderman, O. *Langmuir* **2000**, *16*, 2469.
(20) Waterman, K. C.; Turro, N. J.; Chandar, P.; Somasundaran, P. *J. Phys. Chem.* **1986**, *90*, 6829.
(21) Chandar, P.; Somasundaran, P.; Waterman, K. C.; Turro, N. J. *J. Phys. Chem.* **1986**, *91*, 150.
(22) Somasundaran, P.; Kunjappu, J. T. *Colloids Surf., A* **1989**, *37*, 245.
(23) Soderlind, E.; Stilbs, P. *Langmuir* **1993**, *9*, 2024.
(24) McDermott, D. C.; McCarney, J.; Thomas, R. K.; Rennie, A. R. *J. Colloid Interface Sci.* **1994**, *162*, 304.
(25) Wangnerud, P.; Berling, D.; Olofsson, G. *J. Colloid Interface Sci.* **1995**, *169*, 365.
(26) Sperline, R. P.; Song, Y.; Freiser, H. *Langmuir* **1997**, *13*, 3732.
(27) Kung, K.-H. S.; Hayes, K. F. *Langmuir* **1993**, *9*, 263.
(28) Hanley, H. J. M.; Muzny, C. D.; Butler, B. D. *Int. J. Thermophys.* **1998**, *19*, 1155.
(29) Eskilsson, K.; Yaminsky, V. V. *Langmuir* **1998**, *14*, 2444.
(30) Pagac, E. S.; Prieve, D. C.; Tilton, R. D. *Langmuir* **1998**, *14*, 2333.
(31) Pashley, R. M.; Israelachvili, J. N. *Colloids Surf., A* **1981**, *2*, 169.
(32) Pashley, R. M.; McGuiggan, P. M.; Horn, R. G.; Ninham, B. W. *J. Colloid Interface Sci.* **1988**, *126*, 569.
(33) Kekicheff, P.; Christenson, H. K.; Ninham, B. W. *Colloids Surf., A* **1989**, *40*, 31.
(34) Rutland, M. W.; Parker, J. L. *Langmuir* **1994**, *10*, 1110.
(35) Manne, S.; Cleveland, J. P.; Gaub, H. E.; Stucky, G. D.; Hansma, P. K. *Langmuir* **1994**, *10*, 4409.
(36) Manne, S.; Gaub, H. E. *Science* **1995**, *270*, 1480.
(37) Sharma, B. G.; Basu, S.; Sharma, M. M. *Langmuir* **1996**, *12*, 6506.
(38) Ducker, W. A.; Grant, L. M. *J. Phys. Chem.* **1996**, *100*, 11507.
(39) Aksay, I. A.; et al. *Science* **1996**, *273*, 892.
(40) Wanless, E. J.; Davey, T. W.; Ducker, W. A. *Langmuir* **1997**, *13*, 4223.
(41) Ducker, W. A.; Wanless, E. J. *Langmuir* **1999**, *15*, 160.
(42) Patrick, H. N.; Warr, G. G.; Manne, S.; Aksay, I. A. *Langmuir* **1999**, *15*, 1685.
(43) Fielden, M. L.; Claesson, P.; Verrall, R. E. *Langmuir* **1999**, *15*, 3924.
(44) Schultz, J. C.; Warr, G. G.; Hamilton, W. A.; Butler, P. D. Paper presented at the 73rd American Chemical Society Colloid and Surface Science Symposium: Boston, MA 13−16 June 1999.
(45) Wall, J. F.; Zukoski, C. F. *Langmuir* **1999**, *15*, 7432.
(46) Velegol, S. B.; Fleming, B. D.; Biggs, S.; Wanless, E. J.; Tilton, R. D. *Langmuir* **2000**, *16*, 2548.

silica liquid cell. In a typical experiment, solutions of increasing surfactant concentration were injected sequentially into the cell. It was determined, for each of the surfactants used in this investigation and on each of the substrates, that the order of addition of surfactant does not affect the measured interaction force and that rinsing with water quickly produced a force profile equivalent to curves measured in absence of surfactant. These observations indicate that equilibrium is established quickly in this system. A new cantilever was used for each experiment. Because small variations in spring constant and radius may occur between cantilevers, even from the same batch, the interaction force between each tip and silica surface in the presence of a standard solution of 32 mM dodecyltrimethylammonium bromide at pH 6 and 0.0001 M NaCl was measured. The characteristic maximum repulsive force (magnitude of repulsion where the tip jumps into contact with the surface) under these conditions was used to normalize the interactions between different tip/surface combinations. The absolute values of the maximum repulsion varied by as much as 20% primarily due to small variations in the tip radius. Because the radius of the tip is not precisely known and the application of Derjaguin's approximation with small radius probes is questionable, interaction forces are presented without normalizing by the radius of the probe.

(b) Suspension Stability. Suspension stability was determined by measuring the turbidity of a 0.02 vol % suspension of dense spherical monodisperse silica particles formed by the Stöber process and obtained from Geltech Inc. Mean particle diameter was 250 nm as determined by laser light scattering (Coulter LS230) and surface area determined by nitrogen adsorption (Quantachrome Nova 1200) was 14.6 m^2/g. Turbidity was measured on a Hach model 2100 turbidity meter. Stable suspensions showed minimal decrease in turbidity after 60 min of settling while the turbidity of unstable suspensions decreased significantly due to the more rapid sedimentation of coagulates.

(c) Adsorption. The adsorption of surfactant on the silica particles described above was measured by the solution depletion method. A known concentration of surfactant is mixed with a 5 vol % particle suspension equilibrated and centrifuged to separate the supernatant from the surfactant-coated particles. Residual surfactant concentration was then measured by total organic carbon analysis using a Tekmar-Dohrmann Phoenix 8000 analyzer. To prevent foaming during analysis, all samples were diluted to less than 50 mg/L concentration of surfactant. Known concentrations of surfactant were also measured before and after centrifuging to demonstrate the validity of the method.

(d) Zeta Potential. The zeta potential of the particles was measured using a Pen-Kem Lazer Zee Meter, model 501, based on the principle of electrophoretic mobility. Differential voltage was kept below 200 V to minimize sample degradation. Presented values are the averages of at least six measurements.

(e) Contact Angle. Contact angle was measured between an air bubble and a CVD silica substrate using a Ramé-Hart goniometer, model A100. The angle of the substrate was adjusted to within 5° of the angle at which an approximately 10 μL air bubble placed on the underside of the substrate would not leave the surface. Six values of the advancing contact angle were measured on each of at least three bubbles placed on the surface. The results presented below are the averages of these measurements.

Results and Discussion

Figure 1 depicts the surface forces present between a silicon nitride tip of an AFM cantilever and a mica substrate without surfactant and in the presence of dodecyltrimethylammonium bromide solution (C_{12}TAB, where C_{12} represents the number of carbon atoms in the alkyl chain) at 32 mM at pH 4 with 0.1 M NaCl. All experiments were performed at room temperature. In the absence of surfactant, no repulsive forces are observed, and as the tip approaches the substrate, van der Waals forces cause the surfaces to jump into contact. This behavior was observed regardless of ionic strength or pH on both silica and mica substrates. However, in the presence of surfactant, mica has been shown to be coated with full cylindrical micelles, as mentioned above.[35,36] This was also confirmed in this investigation by imaging the adsorbed micelle layer under these conditions. As a result of this coverage, significant repulsive forces are observed. Note that the average adhesion forces between surfaces without and with surfactant films were not statistically different, indicating that real contact between the tip and surface was made in both cases.

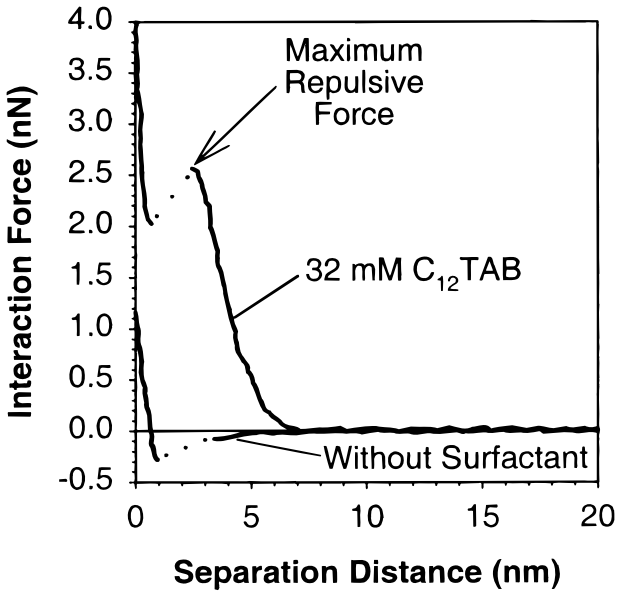

Figure 1. Measured interaction forces between the AFM tip and a mica surface in 0.1 M NaCl solution at pH 4, both with and without 32 mM of C_{12}TAB surfactant. Dotted line indicates the region of mechanical instability where the cantilever "jumps" into contact with the surface. Interaction force curves where repulsion was observed, regardless of solution conditions or substrate material, showed similar features to the interaction in the presence of surfactant. Under conditions where no repulsive forces were observed, the measured force profiles were indistinguishable from the interaction in the absence of surfactant.

The most striking aspect of the force interaction curve in the presence of C_{12}TAB is that at relatively short separation distances, 2.6−7 nm, a strong repulsive force exists between the two surfaces. Then at a particular distance (∼2.6 nm) the repulsion seems to disappear allowing the tip to jump-in and contact the substrate. Although this interaction may at first seem similar to the traditional electrostatic repulsion followed by van der Waals attraction, as described by DLVO theory, it is important to note that because the radius of curvature of the AFM tip is small (10−20 nm) the interaction forces measured in this case are approximately an order of magnitude greater than electrostatic repulsion. Hence, it is proposed that the large repulsion between the two surfaces may be attributed to the elastic deformation of the self-assembled surface surfactant layer followed by its collapse at a specific applied force. A similar process may be observed in bulk micelle systems, where application of hydrostatic pressure leads to annihilation of bulk micelles.[47]

Past analyses of the forces between surfactant-coated surfaces[31−34] have focused primarily on the contributions of electrostatic repulsion and hydrophobicity. In this investigation, by measuring the interaction between a flat

(47) Kaneshina, S.; Shibata, O.; Nakamura, M.; Tanaka, M. *Colloids Surf., A* **1983**, *6*, 73.

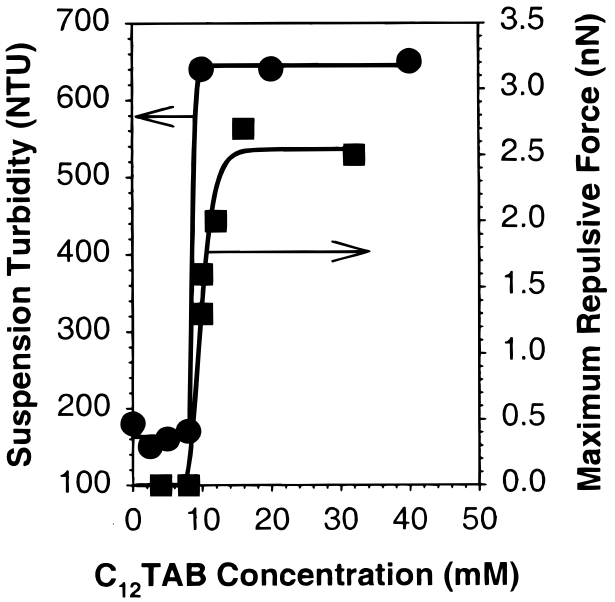

Figure 2. Turbidity in NTU (nephelometric turbidity units) of silica particles after 60 min in a solution of 0.1 M NaCl at pH 4 as a function of C_{12}TAB concentration, and the measured interaction forces between an AFM tip and silica substrate under identical solution conditions. A significant repulsive force arises upon a change in concentration from 8 to 10 mM, which directly corresponds to the formation of a stable suspension.

surface and a very small radius probe, normalized forces were accessed that are much greater in magnitude than those reported in previous investigations.[31−34] Hence, the maximum repulsive force, defined by the force at which the tip jumps into contact with the surface, may be determined. Furthermore, it is important to note that all of the experimental surface interactions described below have similar features at approximately the same distances for a given alkyl chain length, regardless of surface type or solution conditions.

Figure 2 depicts both the suspension turbidity, a measure of stability, of a suspension of silica particles and the surface forces present between the AFM tip and silica substrate as a function of C_{12}TAB concentration at pH 4 and 0.1 M NaCl. Under these conditions, the silica suspension without dispersant is unstable as determined by turbidity measurements. A stable suspension of spherical silica particles showed a minimal decrease in turbidity after 60 min while the turbidity of unstable suspensions reduced by approximately a factor of 4 over the same time period. At high concentrations of surfactant, a large repulsive barrier is observed via surface force measurement and, correspondingly, the surfactant produces a stable suspension.

Stability under relatively high electrolyte concentrations further indicates that electrostatic repulsion, as proposed by previous authors,[31−34,48−53] may not be the only stabilization mechanism at work in this system. In fact, at 32 mM of C_{12}TAB surfactant, silica suspensions were found to be stable even at 5 M NaCl. At this concentration, zeta potential is +2 mV and it is unlikely that electrostatic repulsion plays any significant role in suspension stability. Instead, it is proposed that the steric repulsion arising from the elastic deformation of the self-assembled surfactant films is the dominant repulsion mechanism.

At lower C_{12}TAB concentrations, a different behavior is observed. As the concentration of surfactant is first increased, no change in the attractive force between the tip and surface is observed. The measured force profile does not deviate from the interaction with no surfactant, presented in Figure 1, up to a concentration of 8 mM of surfactant. As shown in Figure 3, at this concentration, the electrophoretic zeta potential is +53 mV (with a saturation level of +61 mV) and the measured adsorption on the particles is 3.2×10^{-6} mol/m^2 (with a saturation at 8.0×10^{-6} mol/m^2) or 40% of saturation adsorption. At saturation, the average area per molecule, assuming a spherical self-assembled surface aggregate, is 42 Å^2/molecule, which compares favorably to 38 Å^2/molecule reported at the air−water interface for similar solution conditions (0.1 M NaCl at 25 °C).[10] By 10 mM C_{12}TAB, where zeta potential is +59 mV and surfactant adsorption is 4.0×10^{-6} mol/m^2 (50% of saturation adsorption), a barrier to agglomeration is observed. Between the same surfactant concentrations, the initially unstable suspension becomes fully stabilized.

The adsorption isotherm and zeta potential measured on the silica particles and the contact angle measured on the silica plate as a function of C_{12}TAB concentration are presented in Figure 3. These measurements were performed in order to elucidate the structure of this surfactant film over the region of stability transition and determine its proximity to known concentrations of previously reported structural transitions. Figure 4 shows pictorially the possible structures existing on the silica surface at concentration ranges corresponding to letters A−F in Figure 3. As surfactant is introduced to the system, it has been shown to first adsorb as individual surfactant molecules.[11] However, at the critical hemimicelle concentration lateral interactions between the alkyl chains of the surfactant molecules begin to increase the affinity of the molecules for the surface and adsorption occurs more rapidly. In the present system, from 0.007 to 20 mM C_{12}TAB, the adsorption isotherm is linear, indicating that at this salt concentration the critical hemimicelle concentration is less than 0.007 mM and that hemimicelles are present on the surface at even the lowest measured concentrations. This is depicted in Figure 4 as individual surfactant adsorption at some concentration below 0.007 mM (A) and as a mixture of hemimicelles and individually adsorbed surfactant molecules at concentrations around (B).

Up to a concentration just below 0.1 mM of surfactant, these adsorbed hemimicelles have little effect on either the surface hydrophobicity or zeta potential, most likely due to their low concentration on the surface (less than 2% of the theoretical monolayer coverage, 4.37×10^{-6} mol/m^2).

At and above 0.1 mM the adsorbed surfactant increases hydrophobicity and generates a positive zeta potential. This reversal of zeta potential is commonly explained by the formation of bilayer patches at the surface.[16,17] However, in this system the hydrophobicity of the surface continues to increase despite the now positive surface potential. Hence, zeta potential reversal is more likely a result of enhanced adsorption due to either hydrophobic association during hemimicellization or specific adsorption. These structures, which are expected to exist up to the maximum value of hydrophobicity (approximately at 2.3 mM), are shown pictorially as (C) in Figures 3 and 4. At the maximum in hydrophobicity, indicating the con-

(48) Sato, T.; Kohnosu, S. *J. Colloid Interface Sci.* **1990**, *143*, 434.
(49) Huang, L.; Somasundaran, P. *Colloids Surf., A* **1996**, *117*, 235.
(50) Ducker, W. A.; Luther, E. P.; Clarke, D. R.; Lange, F. F. *J. Am. Ceram. Soc.* **1997**, *80*, 575.
(51) Colic, M.; Fuerstenau, D. W. *Langmuir* **1997**, *13*, 6644.
(52) Fuerstenau, D. W.; Colic, M. *Colloids Surf., A* **1999**, *146*, 33.
(53) Solomon, A. M.; et al. *Langmuir* **1999**, *15*, 20.

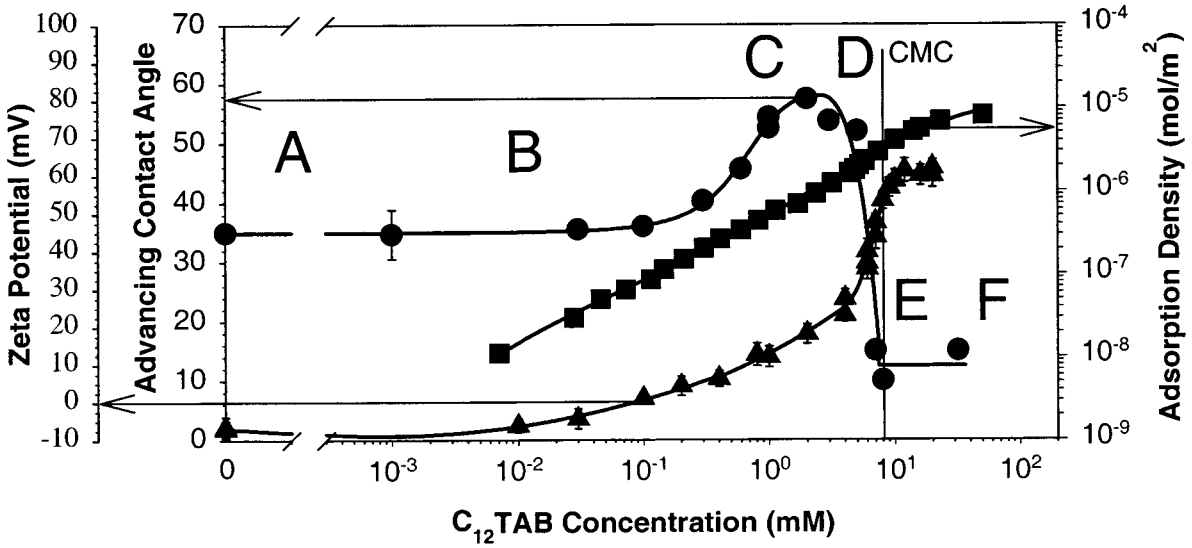

Figure 3. Adsorption isotherm (squares), zeta potential (triangles), and contact angle (circles) of the silica surfaces, in 0.1 M NaCl at pH 4 as a function of solution C_{12}TAB concentration. In the region where the system becomes stabilized by the surfactant, no significant change in the trends of the measured values is observed. The onset of surface forces in this system seems to occur after bilayer or surface micelle formation has started but is still far below the concentration where saturation adsorption is achieved. The bulk cmc also does not correspond to this transition point.

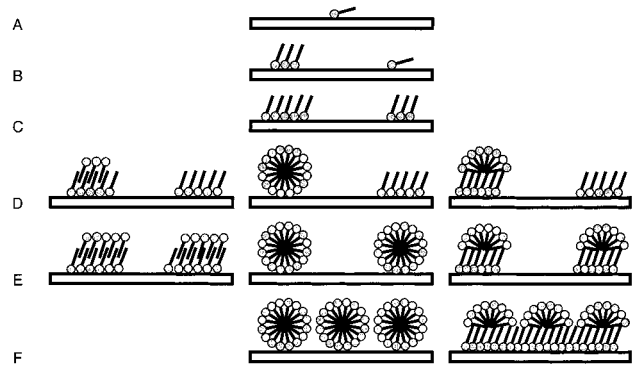

Figure 4. Pictorial depictions of the possible self-assembled surfactant films at concentration ranges corresponding to A−F in Figure 3: (A) individual surfactant adsorption; (B) low coverage of hemimicelles; (C) higher coverage of hemimicelles; (D) coexisting hemimicelles and bilayers, spherical surfactant aggregates, or monolayers with semispherical caps; (E) bilayers, spherical surfactant aggregates, or monolayers with semispherical caps at less than full surface coverage; (F) spherical surfactant aggregates or monolayers with semispherical caps at full surface coverage.

centration at which the maximum number of alkyl groups are oriented toward the solution, yields an adsorption of 10^{-6} mol/m^2 or 23% of theoretical monolayer coverage. It is this relatively low coverage that results in a maximum contact angle (57°) significantly less than that expected for a fully hydrophobized surface (>90°).

Between 2.3 and 6 mM (23−53% of theoretical monolayer coverage) hydrophobicity significantly decreases, and after 6 mM, zeta potential begins to increase at a more rapid rate. This significant increase in the rate of zeta potential rise and rapid decrease in hydrophobicity indicates that an increasing number of trimethylammonium moieties are oriented toward the solution (reverse surfactant orientation). Of critical importance, at these concentrations, is the self-assembled structure that allows this orientation. Traditionally, bilayers have been proposed,[16,17] but from images of the surface at higher concentrations (32 mM), spherical self-assembled surface aggregates are observed. A recent series of papers,[54−55] based on thermodynamic criteria only, has also suggested that the observed images could actually be semispheres on top of perfect monolayers. It should be noted that these thermodynamic predictions ignore the unfavorable contributions of the hydrophobic edges of the monolayers and the area between close-packed semispheres on the monolayer surface, both of which are exposed to the aqueous solution in this structure. Critical to understanding the onset of repulsion and suspension stability is determination of the intermediate structures that form between hemimicelles and the aggregates observed at higher concentrations.

In the concentration range corresponding to (D), there is a gradual decrease in hydrophobicity. This suggests that the transition to a structure with a reversed surfactant orientation is not sudden but that spherical self-assembled aggregates, bilayers, or monolayers with semispherical caps coexist with hemimicelles in this concentration range. These possible structures are depicted in (D) in Figure 4.

At the critical micelle concentration (cmc) under these conditions (8.0 mM) no significant change in the zeta potential, adsorption, or hydrophobicity trends occurs, indicating that it is the residual monomer concentration that primarily influences the structure at the surfaces.[13] On silica, at 7 mM the contact angle is at its minimum value and at 10 mM the zeta potential has saturated. These observations indicate that in this concentration range, either spherical self-assembled aggregates, bilayers, or monolayers with semispherical caps are the only existing structures (Figure 4(E)) even though the surface, at 10 mM for instance, would be only approximately 45% covered by such structures. As concentration is further increased, more of these aggregates are expected to form until concentrations are reached where they may be directly observed via atomic force microscopy (Figure 4(F)). Since spherical structures are observed in this systems at these concentration ranges, it may be assumed that the surface aggregates are either spherical or monolayers with semispherical caps at these concentrations.

Between 8 and 10 mM, a repulsive surface force as well as suspension stability is first observed even though the

(54) Johnson, R. A.; Nagarajan, J. R. *Colloids Surf., A* **2000**, *167*, 31.
(55) Johnson, R. A.; Nagarajan, J. R. *Colloids Surf., A* **2000**, *167*, 21.

formation of structures with reverse surfactant orientation is suspected to form at concentrations as low as 2 mM. The transition between attractive and repulsive forces, instability and stability, over a change in concentration of 2 mM surfactant does not correspond to the structural changes reported by previous authors.[11−34] Hence alternative explanations need to be considered.

There are at least two possible mechanisms that could result in this behavior. Initially a critical point indicating the restructuring of the self-assembled surfactant film was hypothesized. For instance, a transition from a bilayer to true surface micelles or a liquid-like to solid-like transition of the hydrophobic core of these structures could occur. However, analysis of the measurements reported in Figures 3 and 4 as well as preliminary investigation using polarized ATR-FTIR, to be reported in a future publication, have indicated that a transition to a more rigid self-assembled structure such as the spherical aggregates may not be the only mechanism acting in the system. A second possibility is that at lower concentrations the self-assembled surfactant aggregates are not present in large enough quantity and hence do not result in repulsive forces because they can possibly be laterally displaced by the force associated with an approaching AFM tip. As saturation is approached, the mobility of these structures could be substantially reduced forcing the approaching tip to puncture the self-assembled surfactant aggregates resulting in repulsive forces and the stabilization of particulates in suspension.

Controlling the Strength of Self-Assembled Surfactant Films. It is expected that the strength and formation of these surfactant films should be analogous to bulk micelles. The stability of micelles in bulk solution is directly related to the slow micellar relaxation time, τ_2. Aniansson and co-workers,[56] via the pressure-jump technique, measured the stability of a series of sodium alkyl sulfates and found an increase in micellar stability as the chain length was increased from C_{10} to C_{16}. This increase was attributed to increased hydrophobic bonding between alkyl chains that occurs with longer hydrocarbon chain lengths. The maximum repulsive forces as a function of alkyl chain length for C_xTAB (x = 10, 12, 14, and 16) on mica at twice the critical bulk micelle concentration of the respective surfactants are shown in Figure 5. The maximum repulsive force increases linearly over the range of chain lengths measured, indicating a direct correlation between the stability of bulk micelles and the resistance to compression of the self-assembled surfactant surface structures. This also provides further evidence that it is the resistance to deformation of the surfactant films themselves that provide the majority of the repulsive energy barrier to agglomeration.

Octyltrimethylammonium bromide (C_8TAB) was also investigated. However, no repulsive force and no image of surface micelles could be observed at twice the bulk critical micelle concentration (280 mM). If the linear dependence of the maximum repulsive force is extrapolated back to a chain length of eight carbon units, the value of the maximum compressive force approaches zero. Zeta potential measurements of a mica slurry under these solution conditions showed that the net zeta potential increases from −86 mV without surfactant to +21 mV in the presence of C_8TAB. This indicates that self-assembled surfactant aggregates do indeed form on the surface but that these structures are not capable of producing a detectable steric barrier.

(56) Aniansson, E. A. G.; et al. *J. Phys. Chem.* **1976**, *80*, 905.

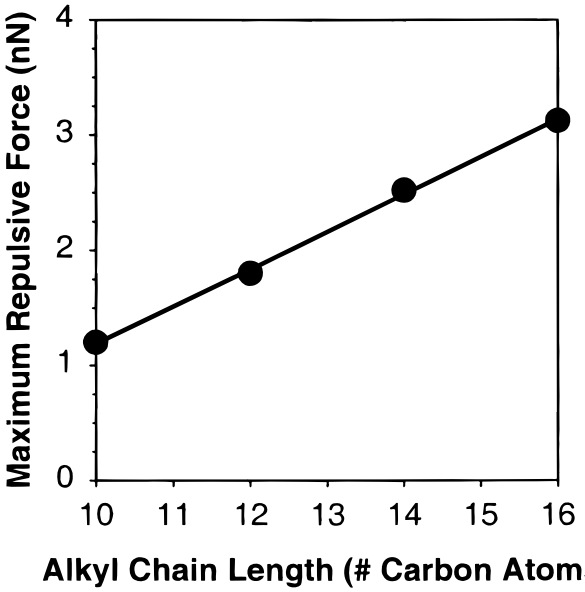

Figure 5. Maximum repulsive force between an AFM tip and mica surface in deionized water as function of alkyl chain length of C_xTAB surfactant at twice the cmc of the surfactant molecules (136 mM, x = 10; 32 mM, x = 12; 7.2 mM, x = 14; 1.84 mM, x = 16). Repulsive force increases as the hydrophobic bonding between surfactant molecules increases.

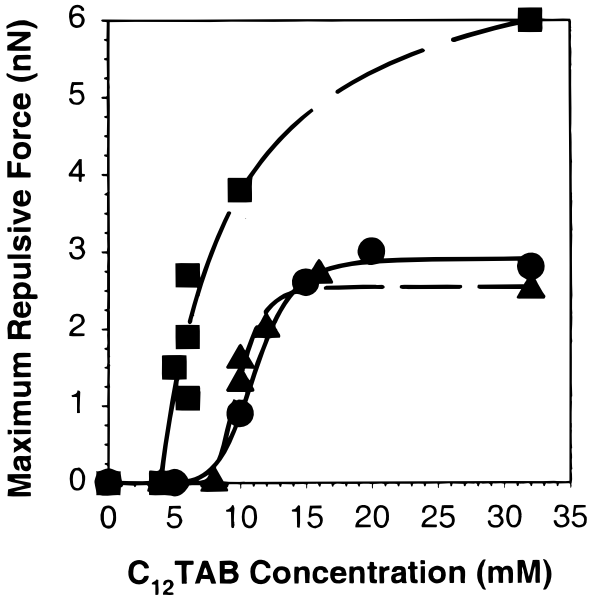

Figure 6. Maximum repulsive force as a function of C_{12}TAB concentration in pH 4 solution between an AFM tip and a mica substrate without additional electrolyte (circles and solid line), with 0.1 M NaCl (squares and long dashed line), and a silica substrate with 0.1 M NaCl (triangles and short dashed line). The magnitude of the repulsive force and concentration at which they arise are dependent not only on solution conditions but also on the substrate material.

Further correlation of the stability and formation of bulk micelles and the self-assembled surfactant surface structures is provided in Figure 6, where the maximum repulsive forces at pH 4 on mica with and without the addition of 0.1 M NaCl are presented as a function of C_{12}TAB concentration. Similar to the increase in alkyl chain length, addition of electrolyte decreases the bulk cmc and increases the slow micellar relaxation time. For the conditions in this investigation the cmc of C_{12}TAB, as determined by surface tension, was reduced from 16 mM with no additional electrolyte to 8.0 mM in the presence

of 0.1 M NaCl. The difference in the onset of the barrier to agglomeration produced by the self-assembled surfactant films with and without electrolyte in solution mirrors this behavior. Without electrolyte, 10 mM of surfactant results in strong repulsive surface forces, whereas with electrolyte, 5 mM is sufficient. Additionally, the magnitude of the repulsive force at a given surfactant concentration is greater at the higher electrolyte concentration.

These results indicate the similarity of bulk micelle formation and stability with self-assembled surfactant films. Note that for the mica surface the strong repulsive force in both electrolyte conditions is observed at concentrations where there are no micelles present in the bulk. Hence, the surfactant structures on the surface are not just micelles adsorbed from the bulk but are actually catalyzed by the substrate. The effect of the surface may be further considered by examining the barrier formation on silica compared with mica under equivalent solution conditions.

Figure 6 also depicts the maximum repulsive force on silica under the identical solution conditions of pH 4 and 0.1 M NaCl as the mica substrate. The effect of the two different substrates is significant. Mica not only has a lower critical concentration at which repulsive force is first observed but also produces significantly greater repulsive forces at a given concentration than the silica surface, possibly due to the different atomic structures of the two substrates which in turn result in different surfactant surface structures (cylindrical surface micelles on mica compared to spherical on amorphous silica). It is interesting to note that the onset of the repulsive forces seems to occur very near or just after the cmc in the case of silica whereas on mica they arose significantly below the bulk cmc. Hence, the behavior of these self-assembled structures follows the trends in bulk micellization (as do hemimicelles); however, the two phenomena are not inherently identical.

In bulk micellization processes, the addition of cosurfactants has been shown to reduce bulk cmc and enhance the stability of micelles.[57−58] Figure 7 shows the dependence of the maximum repulsive force on mica in the presence of C_{12}TAB at 32 mM (twice bulk cmc) as a function of anionic sodium dodecyl sulfate (SDS) concentration. It has been proposed that oppositely charged surfactant incorporates itself into micelles and, by reducing the repulsion between the ionic groups, increases stability and lowers the bulk cmc.[14] A similar process can be expected to occur at the surface. A significant increase in the stability and maximum repulsive force of the surfactant film is observed in the presence of anionic surfactant (e.g., SDS, see Figure 7). It has also been suggested that the maximum in two-dimensional film stability and packing results from a 1:3 molecular ratio (33 mol % SDS) due to hexagonal close packing at the interface.[59] The maximum repulsive force does seem to plateau near this value. However, precipitation occurred before the predicted optimum concentration was reached.

The increase in maximum repulsive force as a function of SDS concentration demonstrates the ability of a cosurfactant to further stabilize self-assembled surfactant surface structures. However, as depicted in Figure 8, very small additions of SDS were observed to have a dramatic effect on the formation of the surfactant surface structures.

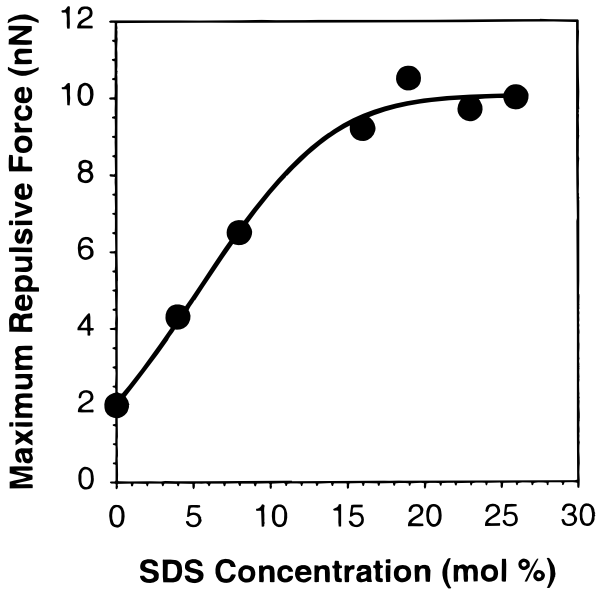

Figure 7. Maximum repulsive force between an AFM tip and mica substrate in deionized water with 32 mM C_{12}TAB as a function of SDS concentration. Before precipitation occurs, the addition of a cosurfactant significantly increases the magnitude of the repulsive force interaction.

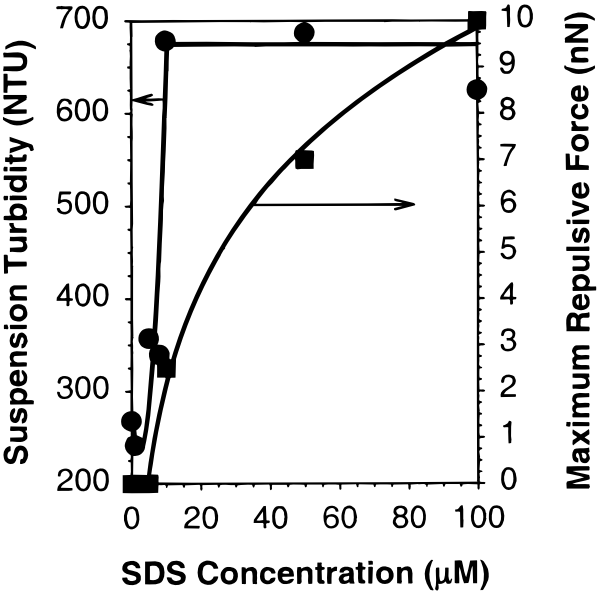

Figure 8. Turbidity of a 0.02 vol % suspension of sol−gel derived 250 nm silica particles after 60 min in a solution of 0.1 M NaCl at pH 4 with 3 mM C_{12}TAB concentration as a function of micromolar SDS addition and the measured interaction forces between an AFM tip and silica substrate under identical solution conditions. Extremely small additions of a cosurfactant that selectively partitions to the solid/liquid interface may significantly reduce the concentration of primary surfactant needed to create repulsive forces between surfaces and stabilize a particulate suspension.

Figure 8 shows the correlation of suspension stability of silica particles with the maximum repulsive force measured against a silica plate in the presence of 3 mM C_{12}TAB and 0.1 M NaCl at pH 4 as a function of micromolar addition of SDS. At 5 μM SDS addition, no repulsive force is observed between the surfaces, but at 10 μM SDS, a strong repulsive force has developed which continues to increase with SDS concentration. Correspondingly, over an identical range of SDS concentration, the initially unstable suspension becomes stabilized.

(57) Scamehorn, J. F. In *Phenomena in Mixed Surfactant Systems*; Scamehorn, J. F., Ed.; American Chemical Society: Washington, DC, 1986; Chapter 1.
(58) Patist, A.; Huibers, P. D. T.; Deneka, B.; Shah, D. O. *Langmuir* **1998**, *14*, 4471.
(59) Shah, D. O. *J. Colloid Interface Sci.* **1971**, *37*, 744.

The abnormally low concentration of SDS needed to form the surface surfactant structures may be explained by the preferential adsorption of SDS at the silica interface. Adsorption experiments, using total organic carbon analysis to determine the total amount of adsorbed surfactant, and inductively coupled plasma spectroscopy, to determine the SDS concentration through the sulfur emission line, have shown that nearly all the SDS added adsorbed at the solid/liquid interface. Hence, the molecular ratio at the interface was estimated to be on the order of 1:10 instead of 1:100 in bulk solution. This is particularly interesting because it was found that no measurable quantity of SDS adsorbed on silica in absence of the C_{12}TAB. Additionally, since little SDS is present in solution, the system is far below bulk cmc and yet strong repulsive forces are once again observed.

The use of cosurfactants or other coadsorbing reagents is a critical factor in the utility of a surfactant dispersant in industrial processes. Not only may the concentrations for effective stabilization be reduced, but many other options can become available to control the overall dispersion of single and multicomponent suspensions. Availability of these engineered dispersants systems can enhance the processing of nanoparticulate suspensions for emerging specialized end uses.

Summary

Stabilization of aqueous particulate suspensions is critical to many industrial operations, which require processing in extreme environments such as high ionic strength, low or high pH, high force, and high shear rates where traditional stabilization methods may not be adequate. Adsorbed surfactant aggregates were found to be effective dispersants under such conditions. It was also determined that the charge reversal process was not sufficient to produce a stable suspension in 0.1 M electrolyte solution. Instead, elastic deformation of adsorbed surfactant aggregates was proposed as the primary stabilization mechanism at high ionic strength. Additionally, the formation of a repulsive barrier was found not to correspond directly to the critical hemimicelle concentration or to the bulk critical micelle concentration. Instead, it appears at a concentration greater than the critical hemimicelles concentration but either below or just above the bulk cmc depending on the nature of the substrate. Possible mechanisms for this sudden appearance of repulsive forces include either a restructuring of the self-assembled surface surfactant layer or a partial saturation of the surface resulting in limited mobility of the surfactant structures. The effect of alkyl chain length, electrolyte concentration, cosurfactant addition, and substrate on this concentration and the magnitude of the repulsive force demonstrates the similarities between these self-assembled surfactant surface structures and the formation and stability of bulk micelles.

Acknowledgment. The authors acknowledge the contributions of Scott Brown for his experimental assistance as well as the financial support of the Engineering Research Center (ERC) for Particle Science and Technology at the University of Florida, The National Science Foundation (NSF) (Grant Numbers EEC-94-02989 and NSF-CPE 8005851), the Industrial Partners of the ERC, and ICI Surfactants for support of this research.

LA000363C